Vol. 594: 65–83, 2018
https://doi.org/10.3354/meps12501

MARINE ECOLOGY PROGRESS SERIES
Mar Ecol Prog Ser

Published April 26

Mechanisms of stability of rhodolith beds: sedimentological aspects

Kyle R. Millar, Patrick Gagnon*

Department of Ocean Sciences, Ocean Sciences Centre, Memorial University of Newfoundland, St. John's, Newfoundland and Labrador A1C 5S7, Canada

ABSTRACT: Rhodolith beds are highly diverse benthic communities organized around the physical structure and primary productivity of red coralline algae. Despite a worldwide distribution and growing recognition that rhodolith beds are important calcium carbonate ($CaCO_3$) bio-factories, little is known of the factors and processes that regulate their structure, function, and stability. One prevalent, largely untested paradigm is that beds develop in environments where water motion is strong enough to prevent burial by sediments. Observations over 7 mo and 3 wk in the centre and near the upper and lower margins of a Newfoundland (Canada) rhodolith *Lithothamnion glaciale* bed, as well as a laboratory mesocosm experiment with rhodoliths and dominant macrofauna from the bed, were used to characterize, parse, and model spatial and temporal variation in rhodolith sediment load (RSL) and movement among presumably important abiotic and biotic factors. RSL and rhodolith movement were largely mediated by a few dominant benthic invertebrates. Hydrodynamic forces were insufficient to move rhodoliths. Daisy brittle stars *Ophiopholis aculeata* and small common sea stars *Asterias rubens* contributed to dislodgement of sediment from rhodoliths. Large green sea urchins *Strongylocentrotus droebachiensis* easily moved rhodoliths in mesocosms. Results provide the first quantitative demonstration that rhodolith beds need not be exposed to threshold hydrodynamic forces to avoid burial. Beds can simply occur in areas where burial is unlikely because of low sedimentation rates. In such cases, select resident bioturbators operating simultaneously at different spatial scales (within and outside rhodoliths) appear to suffice to maintain RSL below lethal quantities, contributing to stability of beds.

KEY WORDS: Rhodoliths · Sedimentation · Bioturbation · Hydrodynamic forces · Urchins · Macrofauna · Cryptofauna · Mesocosm experiments

INTRODUCTION

Sedimentation is the deposition of suspended organic and inorganic particles (sediments) settling out of a water column onto a surface (Wright et al. 2001, Julien 2010, Twichell et al. 2010). Marine sediments are an important food source for detritivores and filter feeders in benthic environments, and their accumulation can create nutrient-rich depositional layers providing habitat and shelter (Dearborn et al. 1981, Hall 1994). However, sessile benthic organisms, in particular primary producers such as seagrasses and macroalgae, are vulnerable to excessive sedimentation, occluding feeding and photosynthetic structures or interfering with recruitment, growth, nutrient uptake, and gaseous exchange (Thomsen & McGlathery 2006, Cabaço & Santos 2007, Riul et al. 2008). Smothering or burial by sediments can be reduced or avoided when physical factors such as water flow or organisms remove or re-suspend sediments (Scheffer et al. 2003, Hinchey et al. 2006, de Boer 2007). Bioturbation, broadly defined as transport processes carried out by animals that directly or indirectly affect sediment matrices, including particle reworking and burrow ventilation, is a widespread phenomenon that helps maintain biologically sustainable sedimentary

*Corresponding author: pgagnon@mun.ca

balances in benthic systems (Dahlgren et al. 1999, Kristensen et al. 2012, Chen et al. 2016). Yet, increasing frequency and intensity of wind and wave storms, as well as accelerating coastal development, affect near-shore sediment transport and increase the likelihood of burial and loss of benthic primary producers (Stocker et al. 2014).

Rhodoliths are red, benthic, non-geniculate coralline algae (Rhodophyta: Corallinales, Hapalidiales, and Sporolithales) that grow as free-living nodules (balls, branched twigs, or rosettes) from the low intertidal to depths >150 m in tropical to polar seas (see review by Foster 2001). They are long-lived and slow-growing, with estimated longevities that can exceed 100 yr and highest growth rates of only a few mm yr^{-1} (Bohm et al. 1978, Bosence 1983, Foster 2001). Rhodoliths can form extensive $CaCO_3$ bio-factories, known as rhodolith beds (aggregations), with the largest bed, ~20 900 km^2, along the coast of Brazil (Foster 2001, Amado-Filho et al. 2012). In part because of their high structural complexity, rhodolith beds typically contain highly diverse assemblages of ecologically and economically important invertebrate and fish species (Hinojosa-Arango & Riosmena-Rodríguez 2004, Kamenos et al. 2004a,b, Steller & Caceres-Martinez 2009, Gagnon et al. 2012). The majority of rhodolith studies have focussed on the use of rhodoliths for paleoenvironmental reconstructions, taxonomic classification of algal species forming rhodoliths, distribution and extent of rhodolith beds, and characterization of biological communities within rhodolith beds (Riosmena-Rodriguez et al. 2017 and references within). A handful of studies have focussed on factors and processes that regulate the structure, function, and stability of rhodolith beds, with progress in this area mainly driven by research in the southwestern and eastern Pacific (e.g. Marrack 1999, James 2000, Steller et al. 2003, Basso et al. 2009, Riosmena-Rodríguez et al. 2012, Ávila et al. 2013, Neill et al. 2015), southwestern and northeastern Atlantic (e.g. Kamenos et al. 2004a,b, Martin et al. 2007, Hinojosa-Arango et al. 2009, Amado-Filho et al. 2010, Andrades et al. 2014, Pereira-Filho et al. 2014, 2015), and Mediterranean Sea (Ballesteros 1994, Basso 1998, Piazzi et al. 2002, Klein & Verlaque 2009, Sciberras et al. 2009).

According to Foster (2001), rhodolith beds typically develop in environments where water motion is strong enough to prevent burial by sediment but not so high or directional as to cause destruction or transport out of areas favourable to growth. Although theoretically sound, this paradigm has remained largely untested since its inception over 15 yr ago (but see Hinojosa-Arango et al. 2009). Movement of rhodoliths within a bed, which can also help discharge some of the settling sediments, can be attributed to 2 main factors: hydrodynamic forces and bioturbation (Riosmena-Rodriguez et al. 2017). Hydrodynamic forces include tidal currents, oscillatory waves, and disturbance by extreme wave storms, which presumably affect mainly the upper limit of rhodolith distribution (Tsuji 1993, Marrack 1999, Basso et al. 2009). Bioturbation in rhodolith beds is generally attributed to the activities of a variety of echinoderms and benthic fishes (Prager & Ginsburg 1989, James 2000). The importance of bioturbation in preventing rhodolith burial, and how it may differ spatially within a bed, is relatively unknown and difficult to quantify (Prager & Ginsburg 1989, Piller & Rasser 1996, Marrack 1999, Pereira-Filho et al. 2015). Moreover, the relative importance of the hydrodynamic environment and bioturbation on rhodolith movement is poorly understood and likely differs spatially, temporally, and geographically.

The first published account of the occurrence of rhodolith beds in the northwestern Atlantic dates back to the mid-1960s (Adey 1966), followed by only a handful of studies describing the main coralline species that form rhodoliths and providing a coarse geographical distribution of the beds across this vast region (Adey & Adey 1973, Bosence 1983, Adey et al. 2005, Adey & Hayek 2011). The study by Gagnon et al. (2012) focussing on 2 subtidal beds of the rhodolith *Lithothamnion glaciale* off the coasts of Holyrood and St. Philip's in southeastern Newfoundland, Canada, is the first quantitative analysis of rhodolith morphology, associated cryptofaunal and macrofaunal abundance and diversity, and organization as beds in the subarctic, northwestern Atlantic. Because the bed in St. Philip's is relatively large (~0.25 km^2), extends across a depth range of ~10 to 25 m, and is located at ~300 m from the mouth of a river, it may be under the influence of a broad range of water flows and sedimentological processes (Gagnon et al. 2012). Daisy brittle star *Ophiopholis aculeata* and mottled red chiton *Tonicella marmorea* are the 2 numerically dominant rhodolith cryptofauna, accounting for ~82% of invertebrates in the bed (Gagnon et al. 2012). The former is a suspension feeder, whereas the latter is a grazer, and hence together these organisms likely filter sediments falling out of the water column and scrape the surface of rhodoliths. Dominant macroinvertebrates on the surface of the bed include the common sea star *Asterias rubens* and the green sea urchin *Strongylocentrotus droebachiensis* (Gagnon et al. 2012). By moving on the bed, both species may alter the position of rhodoliths and their

sediment load, therefore possibly acting as bioturbators. Given these characteristics, the rhodolith bed in St. Philip's represents an excellent system to study sedimentological aspects, and gain a better understanding of the factors and processes that affect rhodolith bed distribution and stability in general.

In the present study, 2 surveys in the rhodolith bed in St. Philip's, as well as one laboratory mesocosm experiment with 2 dominant mobile invertebrates from this bed, were used to characterize, parse, and model spatial and temporal variation in rhodolith sediment load and movement among presumably important abiotic and biotic factors. Specifically, one survey tracked and modelled changes in rhodolith sediment load over 7 mo as a function of water flow, sedimentation, and the abundance of dominant rhodolith cryptofauna and macrofauna near the upper and lower margins of the bed. The other survey examined movement of rhodoliths and water flow over 3 wk near the centre and upper and lower margins of the bed. The mesocosm experiment tested the ability of common sea stars and green sea urchins to move rhodoliths. Collectively, these surveys and this experiment were designed to test the hypotheses that: (1) water flow and the abundance of at least a few dominant rhodolith cryptofauna and macrofauna influence the amount of sediment on rhodoliths; (2) rhodolith movement in the bed is inversely related to depth; and (3) sea urchins cause greater rhodolith movement than sea stars.

MATERIALS AND METHODS

Study site

The study was carried out from June to December 2014 in a *Lithothamnion glaciale* bed spanning ~0.25 km^2 across depths of 10 to 25 m off the coast of St. Philip's on the south shore of Conception Bay, Newfoundland, Canada (47° 35′ 30.9″ N, 52° 53′ 35.2″ W; Fig. 1). Rhodoliths in this bed are relatively small (mean length of longest axis: ~6 cm) and predominantly spheroidal (Gagnon et al. 2012) (Fig. 1). Their uneven surface holds high densities (up to ~2000 ind. m^{-2} of bed) of the daisy brittle star and mottled red chiton (Gagnon et al. 2012). Dominant macroinvertebrates moving on the surface of the bed include the green sea urchin and common sea star (Gagnon et al. 2012).

Rhodolith sediment load — Field survey 1

The amount of sediment covering the surface of rhodoliths, hereafter termed 'rhodolith sediment load', and its relationship with abiotic and biotic factors was assessed by tracking changes over 7 mo in (1) the quantity of sediment falling out of the water column; (2) density of dominant, mobile invertebrate macrofauna on rhodoliths; and (3) biomass of dominant rhodolith cryptofauna, at depths of 12 and 20 m within the bed. These depths were chosen because they correspond roughly to the respective upper and lower margins of the bed, with presumed differences in water flow (higher at 12 than 20 m) and sediment load (lower at 12 than 20 m). For simplicity and accuracy, the concept of rhodolith sediment load in the present study refers strictly to the amount of sediment on the surface of rhodoliths at a given point in

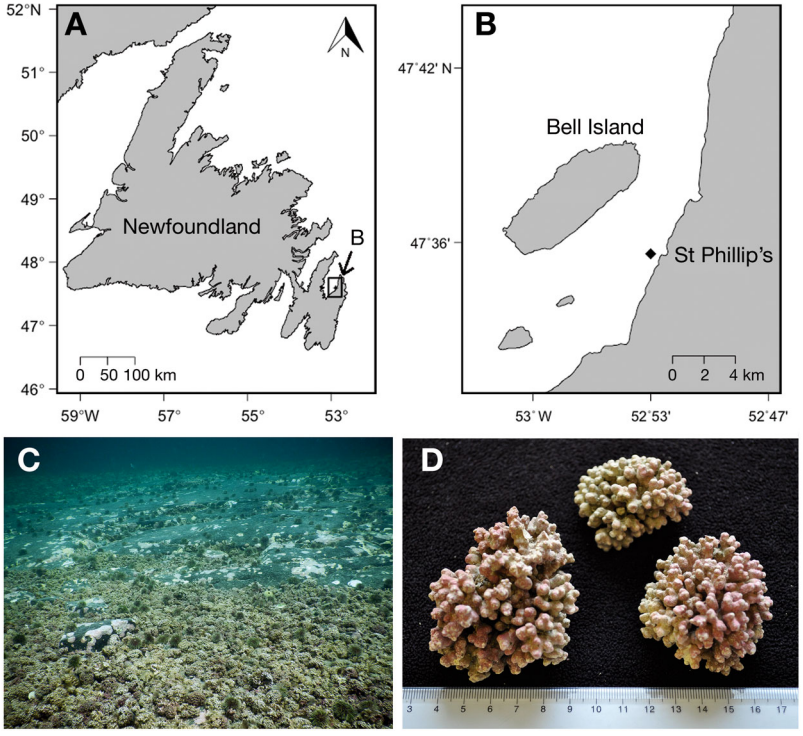

Fig. 1. (A) Newfoundland (eastern Canada) and (B) eastern Conception Bay showing the location of the rhodolith bed (diamond) off St. Philip's. (C) Transition (~5 m across) between green sea urchin *Strongylocentrotus droebachiensis* barrens (upper half of the photo) and the rhodolith *Lithothamnion glaciale* bed (lower half) at a depth of ~10 m (photo by David Bélanger). (D) Size (centimeter scale) and shape (primarily spheroidal) of representative rhodoliths from the bed (photo by Patrick Gagnon)

time. The concept therefore differs from that of 'load' in the geological literature used to describe sediment particles in a flowing fluid either transported along the physical confines of the fluid flow (bed load) or suspended within a given volume of fluid (suspended and wash loads) (Julien 2010).

Sediment load was measured once every 21–40 d (7 times in total) from 11 June to 9 December 2014. On each sampling event, 120 rhodoliths of comparable size were haphazardly hand collected by divers within a large (~50 × 50 m) georeferenced area of the bed at each depth. The present study was primarily concerned with sediment settling out of the water column. Only rhodoliths whose underside was not wedged in sediments and did not release a plume of sediments upon removal from the bed were retained to reduce the likelihood of sampling both benthic and deposited waterborne sediment. Rhodoliths were carefully removed so as not to alter sediment load and transported to the sea surface in large (3.8 l), sealed plastic bags (10 rhodoliths bag^{-1} for a total of 12 bags). Bags of rhodoliths with their water content were transported in large containers filled with seawater to the Ocean Sciences Centre (OSC) of Memorial University of Newfoundland. Upon arrival at the OSC (<5 h after collection), bags were transferred to 330 l holding tanks supplied with ambient flow-through seawater pumped in from a depth of ~5 m in the adjacent embayment, Logy Bay.

The content of each bag was processed using the following procedure. Each rhodolith was vigorously shaken for 30 s within the bag to release sediment in the water. Water and total sediment load from the 10 rhodoliths was then filtered with a vacuum pump (0211-V45F-G8CX; Gast) through a 25 µm filter paper (Grade 114 Wet-Strengthened Qualitative Filter Paper; Whatman). Sediment retained was air dried for 24 h at 60°C in a drying oven (GO1390A-1; Thermo Scientific). Sediment dry weight was then determined by subtracting the original dry weight of the filter paper from the dry weight of the filter paper and its sediment load, as measured with a scale with a precision of ±0.001 g (PB503-S/FACT; Mettler Toledo).

The sampled rhodoliths inevitably differed in shape, size, and orientation on the seabed despite efforts to minimize such variation during collection. As a result, a part of the variation in rhodolith sediment load among the 12 groups of 10 rhodoliths was likely caused by differences in the total amount of rhodolith surface on which sediment settled, with larger rhodoliths likely trapping more sediment than smaller ones. To account for this potential bias and standardize sediment loads, total sediment weight for each group of 10 rhodoliths was divided by the sum of all surface areas of those same 10 rhodoliths. The total surface area of each rhodolith was estimated by relating the length of the longest, intermediate, and shortest axes, measured with a calliper with a precision of ±0.1 cm, with the Knud Thomsen approximation for a general ellipsoid with least relative error (at most 1.061%):

$$S \approx 4\pi\left(\frac{(ab)^p + (ac)^p + (bc)^p}{3}\right)^{(1/p)} \quad (1)$$

where S is the surface area, $p = 1.6075$, and a, b, and c are half the lengths of the longest, intermediate, and shortest axes, respectively (Klamkin 1971). Gagnon et al. (2012) used the lengths of the longest, intermediate, and shortest axes and simple mathematical relationships described by Graham & Midgley (2000) to approximate rhodolith shape in the same bed examined in the present study, and concluded that rhodoliths were predominantly spheroidal. Because calculation of rhodolith surface areas in the present study required greater accuracy, and none of the rhodoliths collected were true spheres, the Knud Thomsen approximation for a general ellipsoid was deemed superior to any other methods of approximation. Bosence (1976) documented considerable variation in patterns of branching and density of branches in maerl from western Ireland. Both traits did not vary appreciably among rhodoliths in the present study (Fig. 1 and Gagnon et al. 2012). Therefore, rhodolith surface area based uniquely on rhodolith physical dimensions were deemed sufficiently accurate for the present study.

Water flow

Water flow velocity, u, v, and w (in the x-, y-, and z-direction, respectively) at the shallow (12 m) station, was measured from 28 July to 7 December 2014 with a Doppler current meter (Vector Current Meter; Nortek). The instrument was attached vertically to a frame anchored to the seabed. Velocity at 5 cm above the rhodolith bed was recorded at a rate of 64 readings min^{-1} during the first 15 min of every hour (for a total of 960 readings h^{-1}). This sampling regime, termed 'burst sampling', is commonly used in oceanographic studies to estimate hydrodynamic conditions over long time scales (Lowe et al. 2005, Thomson & Emery 2014). Velocity in each direction was averaged across each block of 15 min. The resulting 3 mean velocities for each time block were

then averaged into a single, overall, directionless flow speed (Smith 1994).

Only 1 Doppler current meter was available, precluding continuous measurement of flow simultaneously at the deep (20 m) station. To determine whether flow velocity differed between both stations, the instrument was temporarily moved once every 2 or 3 wk (depending on availability) to the deep station. It was left there for ~1.5 h to ensure flow velocity was recorded uninterruptedly over 15 min, and relocated to the shallow station for further recording. The instrument was brought to the OSC once a month for precautionary data readout and maintenance, and redeployed at the shallow station generally within the following 2 or 3 d, resulting in a few data gaps throughout the survey. Water flow at both stations was deemed similar (see Supplement 1 at www.int-res.com/articles/suppl/m594p065_supp.pdf). Accordingly, preliminary investigation of the relationship between water flow and rhodolith sediment load was restricted to the shallow station because of the finer temporal resolution in flow regime available for this station (see 'Statistical analysis' below).

Waterborne sediments

Sediments falling through the water column were collected from 2 May to 7 December 2014, with sediment traps at both stations. Each trap consisted of a 30 cm long PVC pipe with an internal diameter of 5.08 cm and a plastic cap tightly affixed to one end. Accordingly, length was approximately 6 times greater than diameter, which is above the minimum 5:1 ratio to prevent re-suspension of trapped sediments in high-energy wave and current environments (White 1990, Storlazzi et al. 2011). The traps were fastened, open end facing upwards, at a height of 1 m above the bed, to a thin (1.9 cm in diameter) metal rod secured to a 15 kg cinder block placed horizontally on the bed. Four traps located 1 to 4 m from one another were used simultaneously at each station. Every 23 to 40 d, divers tightly capped the open end of all traps and swapped them for empty ones. Traps with sediments were then brought to the laboratory to determine the amount of sediments. The sediment content of each trap was filtered and dried with the same methodology used for determining rhodolith sediment load. Sedimentation rate for each trap was calculated by dividing sediment dry weight by the surface area of the trap aperture (20.3 cm^2) and number of days the trap was at the station (Storlazzi et al. 2011).

Mobile invertebrate macrofauna

Preliminary survey of the rhodolith bed at both stations indicated that green sea urchins and common sea stars were the dominant invertebrate macrofauna moving on the bed. Green sea urchins can move rhodoliths (James 2000), whereas several species of sea stars, including common sea stars, are effective bioturbators on soft-sediment bottoms (Gaymer et al. 2004, Scheibling & Metaxas 2008). Accordingly, both species were chosen to examine the influence of mobile invertebrate macrofauna on rhodolith sediment load. The density of urchins and sea stars at both stations was measured every 19 to 38 d from 11 June to 7 December 2014, with the following procedure. On each sampling day at each station, divers swam with a quadrat (30 × 30 cm) and a digital camera (PowerShot D30; Canon) above the bed over a straight distance of ~75 m. Every 2 or 3 m, the diver holding the quadrat closed his eyes (to avoid bias) and deposited the quadrat on the bed; the quadrat was then photographed. Differences in total distance covered by divers and distance separating consecutive quadrats yielded 20 to 29 photo quadrats on each sampling day at each station. Mean density of each species on each sampling day for each station was determined from visual counts in the photo quadrats of urchins and sea stars with a test diameter (TD) >2 cm and body diameter (BD; length of the longest axis between 2 opposing arm tips) >5 cm (minimum detectable sizes on the imagery), respectively.

Rhodolith cryptofauna

Complementary study of the same rhodolith bed showed that the dominant rhodolith cryptofauna were the daisy brittle star and mottled red chiton, together representing respectively 82 and 78% of the total number and biomass of invertebrates (Gagnon et al. 2012). Juvenile green sea urchins and common sea stars were the next 2 most abundant (density and biomass) cryptofaunal species (Gagnon et al. 2012), which is consistent with preliminary observations in the present study. Accordingly, these 4 species were chosen to examine the influence of rhodolith cryptofauna on rhodolith sediment load. All individuals of these 4 species were extracted with probes and forceps from the same rhodoliths sampled for sediment load.

Most brittle stars were firmly attached to rhodoliths, with the bulk of their body deeply recessed within rhodolith surface cavities, making it virtually

impossible to extract individuals without tearing body parts. Accordingly, biomass of each of the 4 species was quantified because it was deemed a more accurate estimator of their potential influence on sediment load than density. Rhodoliths were fractured into pieces as required to ensure complete biomass extraction. Total wet weight per species of all individuals (whole and fragments) from each of the 12 groups of 10 rhodoliths collected at each station on each sampling event was determined with a scale (same as in the rhodolith sediment load determination described above) with a precision of 0.001 g, and averaged for each group of rhodoliths.

Rhodolith movement in the field — Field survey 2

To check the assumption that rhodolith movement occurs in natural habitats, while testing the hypothesis that movement is inversely related to depth, a 3 wk survey of changes in the location of marked rhodoliths across a depth range of 8 m was carried out at the study site, at ~150 m from both stations in Field survey 1. The survey was partitioned in 3 runs of 5 d each in late fall 2014, when wave action in southeastern Newfoundland typically increases (Brodie et al. 1993) and is more likely to affect the distribution of unattached benthos like rhodoliths: (1) 13 to 18 November (hereafter termed 'mid-November'); (2) 27 November to 2 December (late November); and (3) 2 to 7 December (early December).

On 23 October 2014, divers hand collected ~250 non-nucleated (without an inner core of inorganic material), average-sized rhodoliths at depths of 14 to 18 m. Rhodoliths were transported to the OSC where they were individually weighed, and the length of their longest, intermediate, and shortest axes were measured as explained above. Dimensions of each rhodolith were then aggregated using the spreadsheet TRIPLOT (www.lboro.ac.uk/microsites/research/phys-geog/tri-plot/) developed by Graham & Midgley (2000) from pioneering work by Sneed & Folk (1958) to assign each rhodolith to 1 of 3 major shapes (spheroidal, discodial, or ellipsoidal). Spheroidal rhodoliths weighing between 15 and 35 g and with longest axis between 3 and 6 cm were dried for 36 h at 60°C in a drying oven (GO1390A-1; Thermo Scientific). They were subsequently marked (spray painted bright orange) to facilitate relocation underwater.

Marked rhodoliths were transported back to the study site on 13 November 2014, and deployed at depths of 12 (shallow), 16 (intermediate), and 20 m (deep) according to the following procedure. At each depth, divers created 2 rows of 5 groups of 4 rhodoliths, for a total 20 rhodoliths per row and 40 rhodoliths per depth. The 4 rhodoliths in each group were deposited on top of the rhodolith bed, in a 20 × 20 cm square (with 1 rhodolith per corner) centred in a 50 × 50 cm reference frame to standardize distances among marked rhodoliths. Thin metal rods marked with small pieces of bright colored flagging tape were driven into sediments underlying the bed, at 2 opposing corners of the frame to permanently mark its location and orientation. The frame was moved along the row and deposited every 1 m to lay out the remaining 4 groups of marked rhodoliths and permanently mark each new frame location and orientation with additional metal rods. The second row of rhodoliths was created in the same way and paralleled the other row at a distance of ~2 m.

Each frame and associated rhodoliths was photographed from above with a digital camera (PowerShot D30; Canon) at the beginning and end of each run. The 2 images of the same frame were superimposed and cropped as needed to correct for differences in camera angle with ImageJ v1.48 (Schneider et al. 2012). The net distance between each marked rhodolith's initial and final positions in the imagery was averaged for each group of 4 rhodoliths belonging to a same frame, yielding 40 estimates of rhodolith movement depth^{-1} run^{-1}, for a total of 360 estimates throughout the survey. The same marked rhodoliths and frame locations and orientations were used at all 3 depths in the 3 runs. Preliminary trials indicated that painted and non-painted rhodoliths were equally likely to be contacted by the 2 predominant macrofaunal species in the bed, i.e. green sea urchins and common sea stars (see details in Supplement 2). The survey did not allow differentiating rhodolith movement caused by water flow from those caused by bioturbation, but it tracked changes in marked rhodolith position as a first step to determining if rhodolith movement changed with depth.

Rhodolith movement by dominant macrofauna — mesocosm experiment

Casual observations of dominant macrofauna in the rhodolith bed in St. Philip's (and other beds in Newfoundland) suggested that during movement, green sea urchins, and to a lesser extent common sea stars, moved a few rhodoliths over various distances. To quantitatively demonstrate this phenomenon, while testing the hypothesis that urchins cause

greater rhodolith movement than sea stars, a laboratory mesocosm experiment was carried out in which changes in the location of rhodoliths in the presence or absence of urchins and sea stars were tracked. The 4 treatments tested were: (1) presence of 1 urchin and 1 sea star; (2) presence of 2 urchins; (3) presence of 2 sea stars; and (4) no urchins and no sea stars. The first 3 treatments were designed to isolate and compare any differential effects of sea stars and urchins, whereas the last was used as a control.

The experiment was carried out with spheroidal rhodoliths (3–6 cm in length, longest axis), urchins (4–5 cm TD), and sea stars (10–15 cm BD) hand collected by divers at depths of 10–15 m from the bed in St. Philip's on 18 and 27 November 2014. Organisms were transported to the OSC in large containers filled with seawater and transferred upon arrival (<4 h after collection) to 330 l holding tanks supplied with flow-through seawater pumped in from a depth of ~5 m in the adjacent embayment, Logy Bay. These urchin and sea star size classes were chosen to ensure that all individuals were sexually mature (Nichols & Barker 1984, Himmelman & Dutil 1991, Munk 1992), therefore eliminating potential behavioural differences between mature and non-mature individuals, and because they were the most readily available in the bed at the time of collection. All urchins and sea stars were starved for 1 wk prior to experimentation to standardize hunger and activity levels (Scheibling & Hatcher 2007, St-Pierre & Gagnon 2015). Only urchins and sea stars that clung or moved readily in the tanks, indicating normal activity of the podia, were used.

Trials were carried out in plastic trays (35 × 30 × 12 cm [L, W, H]) submerged below the water surface in 75 l glass tanks (62 × 31 × 43 cm) supplied with ~1 l min^{-1} of flow-through seawater (1 tray $tank^{-1}$; Fig. 2). Perforations (1 cm in diameter) every 1.5 cm along the sides of the trays enabled continuous water exchange between the tray and tank. The bottom of each tray was covered with a 1 cm thick layer of sediment collected near the upper margin of the rhodolith bed in St. Philip's, on top of which 9 rhodoliths were placed in a 3 × 3 grid arrangement, with a distance of ~2.5 cm between adjacent rhodoliths. Each trial lasted 4 h and began with the addition (or not) of urchins and sea stars to each tray. Urchins and sea stars were gently deposited between the first and second, and second and third rhodoliths that formed the middle row of 3 rhodoliths in each grid (Fig. 2). Each tray was photographed from above with a digital camera (PowerShot D30; Canon) at the onset of trials, and every 30 min thereafter until the end. Images were analyzed with ImageJ v1.48 (Schneider et al. 2012) to determine each rhodolith's total movement, defined as the sum of the linear distances moved from one image to the next. Total movement was averaged across the 9 rhodoliths of a same tray.

Trials were conducted in 24 tanks spatially blocked in 6 groups of 4 tanks each. Each tank in each block was randomly assigned 1 of the 4 experimental treatments, enabling 6 independent replicates of each

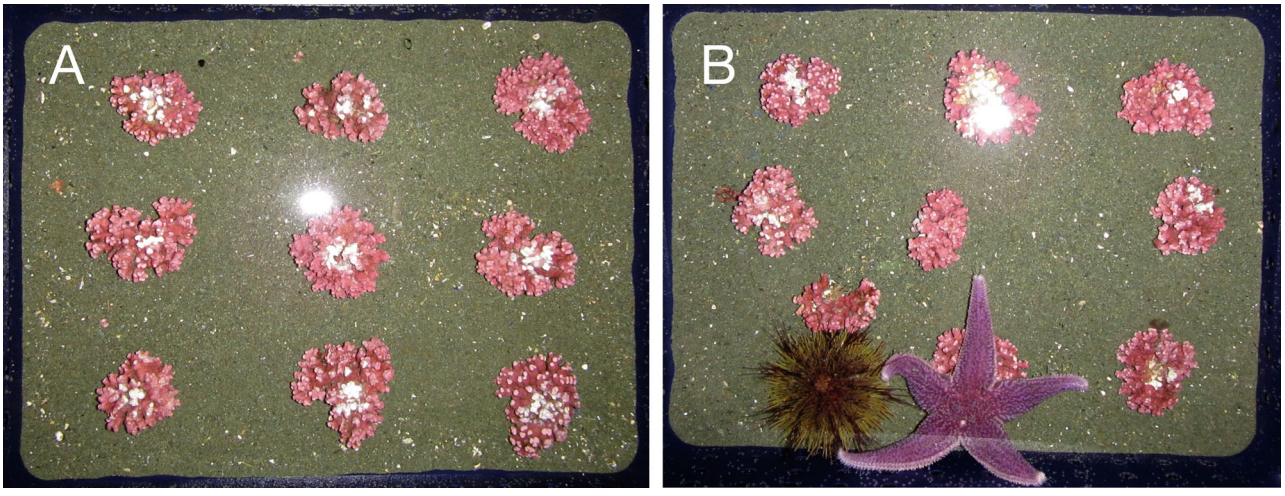

Fig. 2. Experimental set-up used to quantify rhodolith movement by green sea urchins *Strongylocentrotus droebachiensis* and common sea stars *Asterias rubens* (Mesocosm experiment). (A) Location of the 9 rhodoliths on the sediment layer covering the experimental area (35 × 30 cm) prior to adding 1 urchin and 1 sea star in a trial with both organisms. (B) Location of the rhodoliths, urchin, and sea star at the end (t = 4 h) of the same trial. Rhodoliths were marked at the top (white speckles) to facilitate tracking. The white spots in respectively the middle and top of panels A and B are glare from the camera flash used to photograph the experimental area

treatment simultaneously. The experiment was repeated 2 times, with a first run on 25 November and a second run on 4 December, yielding 12 replicates treatment^{-1} (n = 48). Water temperature in the tanks was recorded every 15 min with a temperature logger (HOBO Pendant; Onset Computer). Mean temperature during trials in the first and second runs was 5.2 ± 0.0 and 3.5 ± 0.0°C, respectively. All urchins and sea stars were used only once.

Statistical analysis

Field survey 1

A 2-way ANOVA with the fixed factors Depth (shallow [12 m] and deep [20 m] stations) and Month (the 7 months in which rhodolith sediment load was measured; June to December) was used to test for differences in rhodolith sediment load (RSL) between shallow and deep rhodoliths over time (n = 168). The analysis was applied to the raw data. Six 2-way ANOVAs with the fixed factors Depth (shallow and deep stations) and Month (7 months: June to December 2014) were used to test for differences in density or biomass of dominant rhodolith macrofauna (2 species) and cryptofauna (4 species) between shallow and deep rhodoliths over time (n = 332 or 158 depending on species). These analyses were also applied to the raw data.

Multiple linear regression analysis (Eberly 2007) was used to examine the relationship between RSL and environmental variability. Several stepwise regression models were required to identify the best model fit, as judged by comparing variation (Δ) in Akaike's information criterion (AIC) from one model to the next: the larger the ΔAIC between 2 models, the more dissimilar these models with the best model assigned the lowest AIC (Burnham & Anderson 2004). The AIC was preferred over the Bayesian information criterion (BIC) because the former introduces a smaller penalty term for the number of model parameters, therefore reducing the likelihood of overfitting models. AIC was also deemed more adequate than the corrected AIC (AIC_c) in accommodating the relatively large sample sizes in the models examined (n = 43 to 1445), as recommended by Burnham & Anderson (2004). As per Singer & Willett (2003), a ΔAIC of ≥4 between 2 models was considered a large enough difference to declare both models different in their respective explanatory powers.

Explanatory variables included (or not) in the various models were: (1) significant flow speed (SFS); (2) sedimentation rate (SR); (3) density of adult sea urchins on rhodoliths (DSU); (4) density of adult sea stars on rhodoliths (DSS); (5) biomass of cryptic brittle stars (BBS); (6) biomass of cryptic mottled red chitons (BRC); (7) biomass of cryptic sea urchins (BSU); (8) biomass of cryptic sea stars (BSS); (9) sampling station (S); and (10) sampling month (M). All variables were treated as random, with the exception of S, M, and their interaction, which were treated as fixed. The average of the highest one-third (1/3) of the mean hourly flow speed values recorded over set periods of time, hereafter termed significant flow speed (SFS) per analogy to significant wave height used broadly in oceanographic studies (Pinet 2000), was used in all models that incorporated water flow as an explanatory variable. Accordingly, SFS in the present study is an approximately monthly time-integrated proxy of flow conditions likely to induce the largest variation in RSL.

Because of logistical considerations limiting data collection, the number of observations, and hence sample sizes, varied slightly among sampling stations and months. Two sediment traps were lost at the shallow station in June and data from 1 sediment trap at the deep station in October was omitted because of a likely obstruction to sediment catchment by a dead urchin found in the trap. In most months, DSU and DSS could not be determined from a few low-quality photo quadrats. A few bags of rhodoliths were also lost, precluding measurement of RSL, BBS, BRC, BSU, and BSS (see sample size details in Table S3.1 in Supplement 3). RSL values in the various models were tested against DSU, DSS, BBS, BRC, BSU, and BSS values, which were all measured on the same day as RSL, approximately monthly over the 7 mo period. RSL values were also simultaneously tested against SFS and SR values indicative of water flow and sedimentation in the month or so leading to RSL measurement. For example, shallow RSL values on 3 September 2014 were tested against SFS values (292 values), and average of SR values (4 values), acquired since the previous measurement of RSL on 28 July 2014 (Table S3.1 in Supplement 3). Because replication among factors was uneven (an unbalanced design as per Quinn & Keough 2002), variance among model terms was inevitably heterogeneous. Accordingly, an extension of Welch's test included in the R package Companion to Applied Regression ('car') (Fox & Weisberg 2011) was used to adjust degrees of freedom and protect against increased Type I error (Wilcox 2011).

The explanatory power of SFS on RSL, limited to the shallow station and for the period during which SFS data were available (see 'Water flow' above and Supplement 1 for explanation), was investigated with stepwise regression analysis as a first step to determining the best model fit. SFS was deemed unimportant to RSL, and hence was excluded from further analyses of data from both sites throughout the entire survey (Supplement 4). Stepwise regression analysis with data from both sites throughout the entire survey indicated the best-fitting model to RSL included all candidate variables, except SR (Supplement 4). This model is scrutinized below (see 'Results: Field survey 1').

Field survey 2

A nested ANOVA (Quinn & Keough 2002) with the fixed factor Depth (the 3 depths at which rhodolith movement was quantified: 12, 16, and 20 m), random factor Frame (the 10 frames sampled at each depth) nested within Depth, and fixed factor Run (the three 5 d runs over which rhodolith movement was quantified: mid-November, late November, and early December) was used as a first step to test for differences in rhodolith movement among frames (n = 90). There was no significant effect of the factor Frame nested within Depth ($F_{27,54}$ = 1.296, p = 0.206). Therefore, a 2-way ANOVA with the fixed factors Depth (12, 16, and 20 m) and Run (the three 5 d runs) with data pooled across frames was used to test the effects of depth and sampling period on rhodolith movement (n = 90). Both analyses were treated as particular cases of the generalized linear model (negative binomial) to correct for heteroscedasticity and deviation of residuals from normality detected in the first place with a classical linear model (Venables & Ripley 2002).

Mesocosm experiment

A 2-way ANOVA with the fixed factors Block (the 6 blocks of 4 tanks assigned 1 of the 4 experimental treatments), and Run (the 2 experimental runs with 6 blocks of tanks each) was used as a first step to test for differences in rhodolith movement among experimental blocks and runs (n = 36). There was no significant effect of the factor Block ($F_{5,24}$ = 0.287, p = 0.916) and Run ($F_{1,24}$ = 2.934, p = 0.099). A 1-way ANOVA with the fixed factor Macrofauna (3 out of the 4 combinations of presence and absence of sea stars and urchins) with data pooled across Block and Run was therefore used to test for differences in rhodolith movement by urchins and sea stars (n = 36). Unlike the 3 other treatments, rhodolith movement in the control treatment (no sea stars and no urchins) was null (see 'Results'), potentially artificially influencing the outcome of both analyses. Data from the control treatment were excluded in both analyses to avoid such a bias. These data were instead compared to those from the treatment with the next higher average (presence of 2 sea stars) with a 1-tailed *t*-test (2-sample assuming unequal variances). Both ANOVAs were applied to the raw data.

In all regressions and ANOVAs, homogeneity of the variance and normality of the residuals were respectively verified by examining the distribution of the residuals and the normal probability plot of the residuals (Snedecor & Cochran 1994). In ANOVAs, Tukey HSD multiple comparison tests (comparisons based on least-square means; Sokal & Rohlf 2012) were used to detect differences among levels within a factor. In the analysis of rhodolith macrofauna and cryptofauna, these comparison tests did not detect significant differences in the biomass of daisy brittle stars and mottled red chitons among sampling months identified as significant in the associated ANOVAs (see Fig. 5, Tables S6.3 & S6.4). This outcome is infrequent, yet possible given that post hoc analyses examine pairwise comparisons while ANOVAs examine the difference between all treatment levels. A significance level of 0.05 was used in all analyses. All analyses were carried out in R 3.0.2 (R Core Team 2014). All means are presented with standard errors (mean ± SE) unless stated otherwise.

RESULTS

Field survey 1

RSL varied with depth among months (a significant interaction between the factors Depth and Month; see Table S5.1), ranging from 1.2 ± 0.1 mg sediment cm^{-2} rhodolith in December in deep (20 m) rhodoliths to 5.3 ± 0.6 mg cm^{-2} in September in shallow (12 m) rhodoliths (Fig. 3). It was twice as high (a significant difference) in shallow as in deep rhodoliths at the onset of the survey in June, but otherwise similar at both depths in any given month until the end in December (Fig. 3). There was a similar seasonal trend in RSL at both depths, with a gradual increase from July to September (shallow) or June to August (deep), followed by a steeper decrease until the end (Fig. 3).

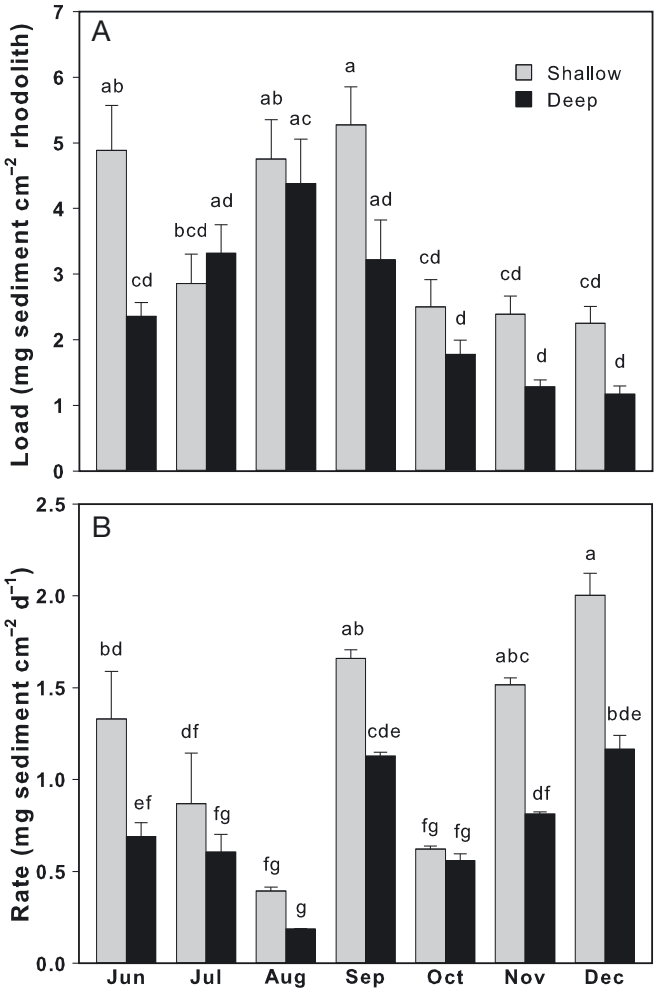

Fig. 3. Mean (+SE) (A) rhodolith sediment load (dry weight) and (B) sedimentation rate (dry weight) at the shallow (12 m) and deep (20 m) stations in the 7 months (June to December 2014) that both variables were measured in Field survey 1. Bars not sharing the same letter are significantly different (LS means tests, $p < 0.05$). In panel (A), n = 12 for each combination of Depth × Month, except at the shallow station in September and November, and deep station in August, with n = 10, 9, and 9, respectively (see Tables S3.1 & S5.1 in the Supplements at www.int-res.com/articles/suppl/m594p065_supp.pdf). In panel (B), n = 4 for each combination of Depth × Month, except at the shallow station in June and the deep station in October, with n = 2 and 3, respectively (see Tables S3.1 & S5.2)

Peak RSL in September at 12 m and in August at 20 m was at least 2 times higher than the lowest RSL values at both depths in December (both differences significant, Fig. 3). SR also varied with depth among months (a significant interaction between the factors Depth and Month; Table S5.2), ranging from 0.19 ± 0.00 mg sediment cm^{-2} d^{-1} in August in deep rhodoliths to 2.00 ± 0.12 mg cm^{-2} d^{-1} in December in shallow rhodoliths (Fig. 3). Yet, preliminary simple linear regression analysis showed there was no relationship between RSL and SR in both shallow ($R^2 = -0.182$, $p = 0.794$) and deep ($R^2 = 0.189$, $p = 0.182$) rhodoliths.

Water flow speed (WFS) in the shallow portion of the bed was generally low throughout the survey, ranging from 0.001 m s^{-1} on 18 October, to 0.301 m s^{-1} on 8 November (Fig. 4). Except for the first part of October when there was a lull, WFS was generally lowest and least variable until the third week of

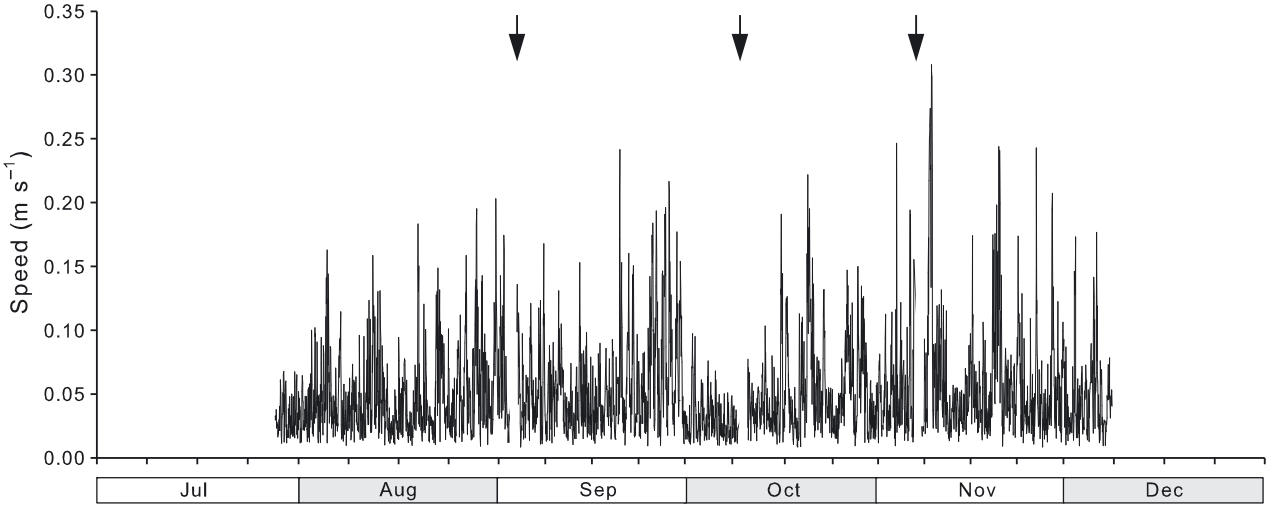

Fig. 4. Water flow speed at the shallow (12 m) sampling station from 28 July to 7 December 2014. Water flow velocity was recorded with a Doppler current meter at 5 cm above the rhodolith bed at a rate of 64 readings min^{-1} during the first 15 min of every hour. Each data point is the average of the 960 readings in the in the *x*-, *y*-, and *z*-direction available for each hour (see 'Materials and methods: Water flow' for details about averaging of flow velocities into dimensionless flow speeds). Data gaps marked by arrows at the top are when the instrument was taken out for data readout and maintenance

August, not exceeding 0.155 m s^{-1}, and gradually increased while becoming more variable until the end of the survey, with at least 6 episodes of a few hours with speeds >0.2 m s^{-1} in November (Fig. 4). WFS in the deep and shallow portions of the bed was similar (Supplement 1).

Analysis of rhodolith macrofauna and cryptofauna showed that the density of large green sea urchins and common sea stars moving on the surface of the rhodolith bed did not vary appreciably throughout the 7 mo survey, though it was respectively 37 and 36% higher in the shallow than deep portions of the bed (Fig. 5A,B; see Tables S6.1 & S6.2). In contrast, biomass of daisy brittle stars, mottled red chitons, and small green sea urchins within rhodolith cavities varied significantly with time and depth independently (Tables S6.3–S6.5). Brittle star biomass peaked in July and December, and was at least 23% lower in the other months. It was also 2 times higher in deep than in shallow rhodoliths (Fig. 5C,D). Chiton biomass was highest in August, September, and December, and 37% higher in deep than in shallow rhodoliths (Fig. 5E,F). Small urchin biomass peaked in June and July, and was twice as high in deep than in shallow rhodoliths (Fig. 5G,H). Biomass of small sea stars within rhodolith cavities did not vary with time or depth (Table S6.6), being generally low throughout the survey (Fig. 5I).

Stepwise regression analyses examining changes in AIC from one model to the next eliminated SFS

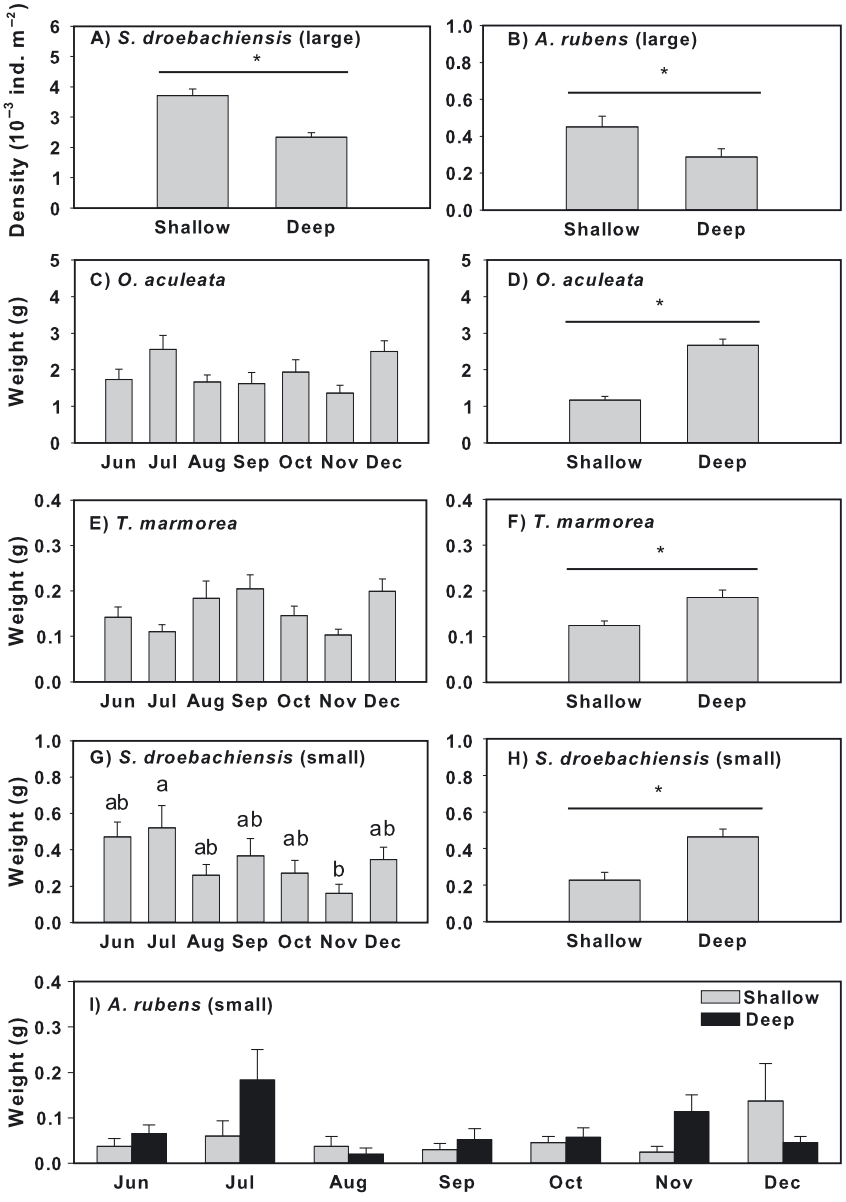

Fig. 5. Mean (+SE) density or wet weight of (A) large green sea urchins *Strongylocentrotus droebachiensis*, (B) large common sea stars *Asterias rubens*; (C,D) daisy brittle stars *Ophiopholis aculeata*; (E,F) mottled red chitons *Tonicella marmorea*; (G,H) small green sea urchins; and (I) small common sea stars on rhodoliths at the shallow (12 m) and deep (20 m) stations in the 7 months (June to December 2014) that rhodolith sediment load was measured in Field survey 1. Bars not sharing the same letter are significantly different (LS means tests, $p < 0.05$; see Supplement 3 for sample sizes across depths and months and Tables S6.1–S6.6 in Supplement 6 for details of statistical analysis for each panel). Post hoc comparisons (LS means tests) did not yield significant differences in pairwise comparisons among sampling months in (C) and (E) despite the significance of Month in the corresponding ANOVAs (see 'Statistical analysis' for additional information about such infrequent outcomes). Letters above bars are therefore not presented in these 2 panels

and SR as explanatory variables of RSL (Supplement 4). The best-fitting model to data from both stations throughout the entire survey was: RSL = DSU + DSS + BBS + BRC + BSU + BSS + S + M + S×M (Supplement 4). This model explained 38% of the variation in RSL ($R^2 = 0.381$, $p < 0.001$). RSL was inversely related to biomass of cryptic brittle stars and small sea stars, yet both factors explained a relatively small proportion (<3%) of the variation in RSL (Table 1). RSL varied significantly between shallow and deep rhodoliths and over time both in the analysis of trends in RSL as mentioned above (Table S5.1; Fig. 3) and in the model relating RSL to environmental variables (Table 1).

Field survey 2

Analysis of data from Field survey 2 showed that movement of marked rhodoliths varied among sampling depths and surveys independently (Table 2). Movement was at least 2.5 times higher in shallow (12 m deep) rhodoliths than in intermediate (16 m) or deep (20 m) rhodoliths (Fig. 6). It was also at least 3.5 times higher in mid-November than in late November and early December (Fig. 6). Instantaneous WFS at 12 m was relatively low, not exceeding 0.2 m s^{-1} across the 3 surveys, and was generally more variable in late November (Table 3, Fig. 7). Mean WFS was similar among the 3 surveys, ranging from 0.039 m s^{-1} in mid-November to 0.044 m s^{-1} in late November (Table 3). However, SFS in late November (0.087 m s^{-1}) was significantly higher than in mid-November, which in turn was similar to SFS in early December (Table 3).

Table 1. Summary of multiple linear regression analysis (applied to raw data) examining the effect of the 8 variables included in the best fitting-model of rhodolith sediment load in Field survey 1. DSU: density of large green sea urchins on rhodoliths, DSS: density of large common sea stars on rhodoliths, BBS: biomass (wet weight) of daisy brittle stars within rhodoliths interstices, BRC: biomass of mottled red chitons within rhodoliths interstices, BSU: biomass of small green sea urchins within rhodoliths interstices, BSS: biomass of small common sea stars within rhodoliths interstices, S: sampling station (shallow [12 m] or deep [20 m]), M: sampling month (June to December 2014) (n = 1461)

Source of variation	df	MS	*F*	p	R^2
DSU	1	9.154	3.78	0.054	0.006
DSS	1	0.041	0.02	0.896	−0.006
BBS	1	0.196	0.08	0.002	0.027
BRC	1	0.397	0.16	0.776	−0.006
BSU	1	24.763	10.24	0.686	−0.004
BSS	1	9.881	4.08	0.045	0.012
S	1	33.526	13.86	<0.001	0.066
M	6	27.987	11.57	<0.001	0.273
S × M	6	5.860	2.42	0.029	0.379
Error	139	2.419			
Corrected total	158				

Table 2. Summary of 2-way ANOVA (generalized linear model with negative binomial distribution) examining the effect of Depth (12, 16, and 20 m) and Run (3 surveys: 1 = mid-November, 2 = late November, and 3 = early December) on movement of marked rhodoliths in Field survey 2

Source of variation	df	χ^2	p
Depth	2	71.453	<0.001
Run	2	118.420	<0.001
Depth × Run	4	3.563	0.468

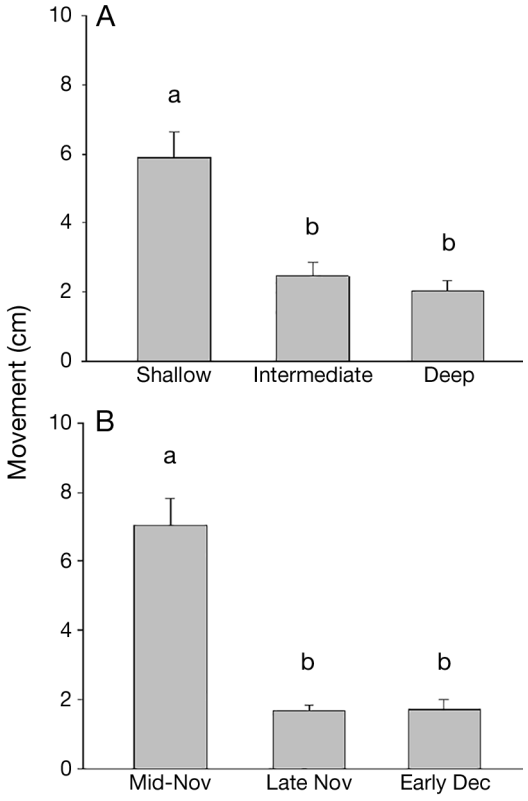

Fig. 6. Mean (+SE) movement of marked rhodoliths (A) over 5 d at the shallow (12 m), intermediate (16 m), and deep (20 m) sampling stations (data pooled across the 3 surveys); and (B) in the 3 surveys: mid-November, late November, and early December (data pooled across the 3 sampling stations), in Field survey 2. Bars not sharing the same letter are significantly different (LS means tests, $p < 0.05$; n = 90 for each bar in both panels; see Table 2 for justification of data breakdown)

Table 3. Mean water flow speed (WFS ± SD), peak WFS, and significant flow speed (SFS ± SD) at the shallow (12 m) sampling station during the 3 late fall surveys in Field survey 2. Water flow velocity was recorded with a Doppler current meter at 5 cm above the rhodolith bed at a rate of 64 readings min^{-1} during the first 15 min of every hour. Each data point is the average of the 960 readings in the in the *x*-, *y*-, and *z*-direction available for each hour (see 'Materials and methods: Water flow' for details about averaging of flow velocities into dimensionless flow speeds). Mean WFS is the average of all hourly speed values. SFS is the average of the highest 1/3 of the speed values. SFS values with the same superscript are not significantly different

Survey	Mean WFS ($m\ s^{-1}$)	Peak WFS ($m\ s^{-1}$)	SFS ($m\ s^{-1}$)
Mid-November	0.039 ± 0.025	0.167	0.066 ± 0.023^{B}
Late November	0.044 ± 0.039	0.200	0.087 ± 0.040^{A}
Early December	0.041 ± 0.028	0.169	0.071 ± 0.027^{AB}
One-way ANOVA[a]	$F_{2,348} = 0.944$, p = 0.390	–	$F_{2,114} = 4.884$, p = 0.009

[a]Both ANOVAs applied to raw data

Mesocosm experiment

Rhodolith movement in the mesocosm experiment varied markedly among the various combinations of presence and absence of common sea stars and green sea urchins (1-way ANOVA: $F_{2,33} = 13.046$, $p < 0.001$). Movement was 46% higher in the presence of 2 urchins than in the presence of 1 urchin and 1 sea star, which in turn was 2 orders of magnitude higher than in the presence of 2 sea stars (Fig. 8). As expected, movement in the absence of sea stars and urchins (control treatment) was null, yet was also vir-

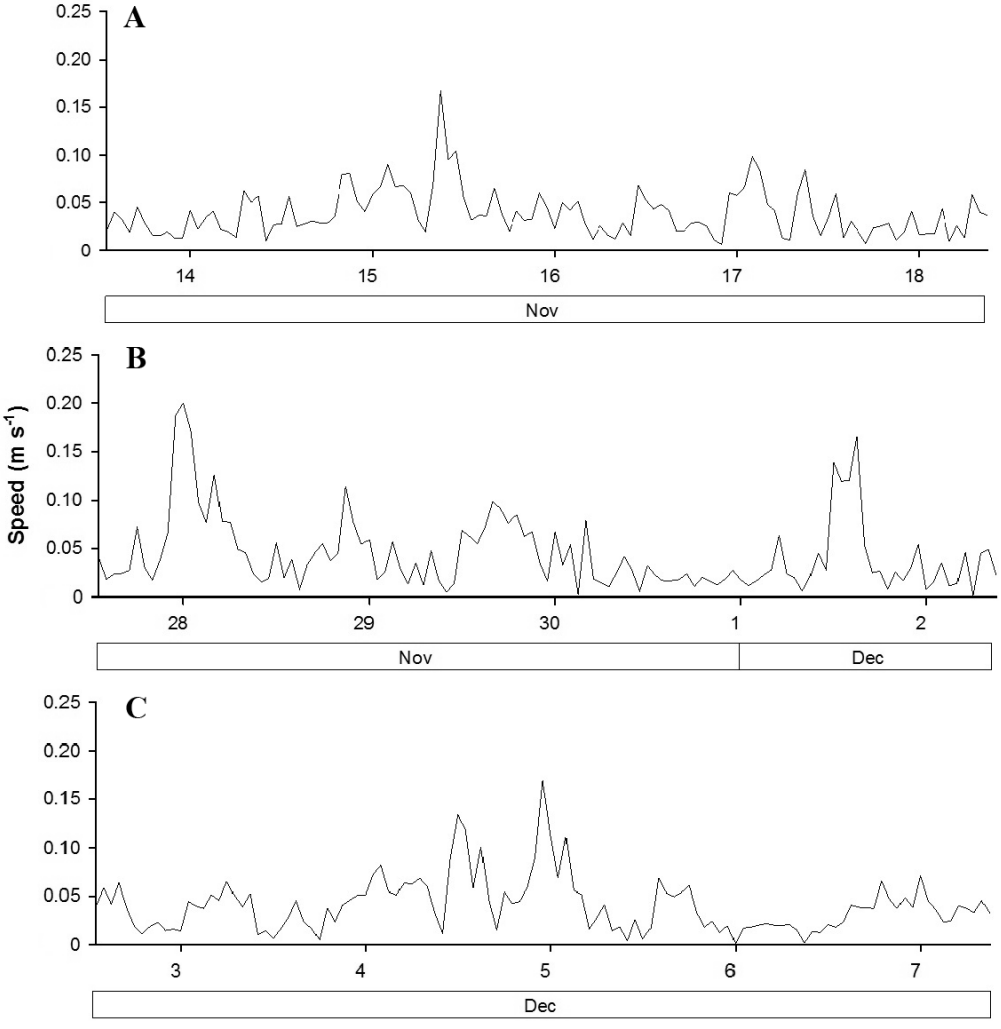

Fig. 7. Water flow speed at the shallow (12 m) sampling station during the 3 late fall surveys in Field survey 2: (A) mid-November (13–18 November 2014), (B) late November (27 November to 2 December), and (C) early December (3–7 December). Water flow velocity was recorded with a Doppler current meter at 5 cm above the rhodolith bed at a rate of 64 readings min^{-1} during the first 15 min of every hour. Each data point is the average of the 960 readings in the *x*-, *y*-, and *z*-direction available for each hour (see 'Materials and methods: Water flow' for details about averaging of flow velocities into dimensionless flow speeds)

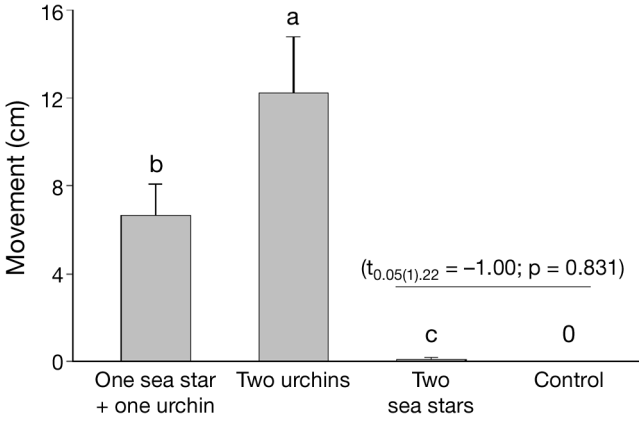

Fig. 8. Mean (+SE) movement of rhodoliths over 4 h in the presence or absence of green sea urchins *Strongylocentrotus droebachiensis* and common sea stars *Asterias rubens* in the mesocosm experiment (control = no urchins or sea stars). Bars not sharing the same letter among the first 3 treatments are significantly different (LS means tests, $p < 0.05$; n = 12 for each bar). A 1-tailed *t*-test was used to compare rhodolith movement between the control treatment (n = 12) and treatment with next higher average (presence of 2 sea stars; see 'Mesocosm experiment' in 'Statistical analysis' and the text in Supplement 1 for details of the analysis)

tually identical to that in the presence of 2 sea stars (Fig. 8), indicating that the ability of sea stars to move rhodoliths was much lower than that of urchins.

DISCUSSION

The 2 field surveys and laboratory mesocosm experiment provide evidence that RSL in the Newfoundland rhodolith bed studied was largely mediated by activities of a few numerically dominant benthic invertebrates. Rhodoliths were distributed across a depth range within which water flow did not vary appreciably, and was likely too weak to induce rhodolith movement that could help remove sediments falling through the water column. Sedimentation appeared too low to bury rhodoliths or to overcome the anti-burial effect of rhodolith movement and surface cleaning by invertebrates. In a seminal review of knowledge about rhodolith biology and ecology, Foster (2001) proposed that control of rhodolith bed distribution lies along a continuum ranging from physical processes such as hydrodynamic forces and sedimentation, to biological processes such as bioturbation. Findings in the present study emphasize the importance of bioturbation over that of hydrodynamic forcing as a mechanism regulating RSL.

Hydrodynamic environment

Rhodoliths in the 7 mo survey (Field survey 1) were sampled at the upper (12 m depth) and lower (20 m) margins of the rhodolith bed because of presumed depth-related differences in water flow regimes potentially affecting RSL. Interestingly, water flow regimes, even during that time of year (September to December) when wave energy typically increases in southeastern Newfoundland (Brodie et al. 1993, Blain & Gagnon 2013, Frey & Gagnon 2016), did not differ between depths. In fact, water flow was generally low throughout the survey, with a few peaks between 0.2 and 0.3 m s^{-1} at 12 m that lasted only a few hours in November. In a study of the relationship between water motion and rhodolith movement in the Gulf of California, Marrack (1999) showed that oscillatory water flow of at least 0.25 to 0.30 m s^{-1} was required to induce rhodolith movement along the shallow (4.5 m) margin of a rhodolith bed. Rhodoliths in the latter study were about half the size of those in the present study, and were more spherical (Marrack 1999). It is therefore unlikely that the predominantly low water flows in the present study caused slight movement, <6 cm in 5 d, of heavier and flatter rhodoliths at 12, 16, and 20 m depths (Field survey 2).

Several findings support the notion that factors other than water flow mediated RSL and movement. First, AIC model selection eliminated SFS and SR as explanatory variables of variation in RSL, retaining only factors containing information about spatial and temporal variation in the abundance of dominant rhodolith cryptofauna and macrofauna (see below). Second, movement of rhodoliths was 3× higher in mid- than late November, yet SFS was significantly higher in late than mid-November. Like water flow, SR was relatively low, <2.3 mg cm^{-2} d^{-1}, throughout the survey at both depths sampled. Regression analysis also showed SR and RSL were unrelated. These results strongly suggest that the bed extends naturally across a depth range where hydrodynamic forces and the amount of sediments falling through the water column do not exceed levels that could alter the physiognomy of the bed via rhodolith fragmentation or burial, and basically switch the system from being biologically to physically driven. In other words, the bed appears to be located in an area where physical forcing was, at least during the 7 mo (June to December) that the survey lasted, a much weaker determinant of rhodolith bed structure and stability than the animals inhabiting the bed.

Steller et al. (2009) reported rapid burial and death of rhodoliths experimentally moved from within to

below the lower margin of a bed in the Gulf of California. This finding is consistent with frequently invoked, but largely untested assumption that rhodolith beds typically develop in environments where water motion or bioturbation are strong enough to move rhodoliths within beds, preventing burial by sediments or biofouling, but not so high as to cause destruction (Steller & Foster 1995, Marrack 1999, Ballantine et al. 2000, Ryan et al. 2007). The present study provides the first quantitative demonstration that beds need not be exposed to threshold hydrodynamic forces to avoid burial. It shows that beds can simply occur in areas where burial is unlikely to occur because of low SRs, in which case select resident bioturbators appear to suffice to maintain RSL below quantities that could alter rhodolith growth and survival (Wilson et al. 2004, Hall-Spencer et al. 2006, Riul et al. 2008).

Bioturbation

Bioturbation (sensu Kristensen et al. 2012) is frequently proposed as a key process generating rhodolith movement (Foster 2001, Riosmena-Rodriguez et al. 2017). However, only a few studies have convincingly demonstrated this process (e.g. Marrack 1999, James 2000, Pereira-Filho et al. 2015). Sea urchins, in particular, are able to carry live and dead rhodoliths on their aboral surface and dig themselves into rhodolith beds, creating pits up to 10 cm deep (James 2000). A similar phenomenon was casually observed at the upper and lower margins of the bed in the present study, with adult-sized (>2 cm TD) green sea urchins slowly plowing rhodoliths while moving on the surface of the bed. The laboratory mesocosm experiment demonstrated the considerable ability of adult-sized green sea urchins in moving rhodoliths on a layer of sediments, while showing the near-complete inability of the next most abundant mobile macroinvertebrate in Newfoundland rhodolith beds, the common sea star. Both species use tens of podia in order to move, but unlike the common sea star, green sea urchins also move large numbers of spines as they travel, often bracing them into cracks and crevices to gain purchase (Frey & Gagnon 2016). Moreover, adult-sized common sea stars like those in the present study are considerably larger than rhodoliths, and their 5 arms largely conform to the shape of objects on which they move. Consequently, movement of the latter is on top of multiple rhodoliths simultaneously, which largely prevents rhodolith movement, instead of in between rhodoliths like green sea urchins, which are as large or smaller than rhodoliths and can easily relocate them.

The present study also provides the first quantitative demonstration of differences in the ability of presumed bioturbators to move rhodoliths, while exploring quantitative relationships between RSL and the abundance of bioturbators in rhodolith bed systems. Modelling showed that RSL was inversely related to biomass of cryptic daisy brittle stars and small common sea stars populating rhodolith interstices. However, there was no clear relationship between RSL and biomass of adult-sized common sea stars and green sea urchins. These findings, together with those outlined above, have several important implications. First, bioturbation in rhodolith beds operates at several scales, with cryptofaunal species sometimes playing a greater role than macrofaunal species in modulating RSL. As explained, the best-fitting model for data from both depths sampled excluded WFS and SR as explanatory variables of RSL. In the bed studied, activities of small brittle stars and sea stars appeared sufficient to maintain RSL under good control. Gagnon et al. (2012) estimated the abundance of daisy brittle stars within rhodoliths in the bed studied to be ~900 ind. m^{-2}. Red mottled chiton was the next most abundant rhodolith cryptofauna with ~750 ind. m^{-2} (Gagnon et al. 2012), yet there was no clear relationship between RSL and chiton biomass in the present study. One cryptofaunal species (brittle star) therefore appeared to play a dominant role in regulating RSL, whereas another co-occurring species (chiton) did not, despite being nearly equally abundant. Drolet et al. (2004b) showed that daisy brittle stars often relocate on a daily cycle. Presumably, such frequent movement, together with consumption of mainly waterborne organic sediments trapped with highly motile arms (Drolet et al. 2004a), were enough to swipe uncaught sediments off the surface or rhodoliths.

Second, species can be effective rhodolith bioturbators during certain portions of their life cycle or below threshold rhodolith densities. The mesocosm experiment showed that adult-sized common sea stars did not move rhodoliths while travelling. However, RSL in the field was inversely related to biomass of small, cryptic conspecifics, suggesting that the latter significantly altered RSL in the bed. The experiment also showed that green sea urchins easily moved a few rhodoliths spaced out on a layer of sediment, yet did not affect RSL in the bed. With ~860 rhodoliths m^{-2} (Gagnon et al. 2012), the bed contained a much higher density than in the experiment. Rhodoliths in the bed often formed tight patches of interlocked individuals, and hence movement of rhodoliths by urchins

in the bed was arguably more challenging, and likely less frequent than in the laboratory. Marrack (1999) concluded that bioturbation by fish, including the stone scorpionfish *Scorpaena mystes* is an important mechanism for rhodolith movement in Californian rhodolith beds. The sand tilefish *Malacanthus plumieri* transports and incorporates rhodoliths into sedimentary mounds in Brazilian rhodolith beds (Pereira-Filho et al. 2015). The present study did not examine the effects on rhodolith movement and RSL of 2 fish species frequently encountered in the bed, the winter flounder *Pseudopleuronectes americanus* and the winter skate *Leucoraja ocellata*. Both fish lie on rhodoliths and initiate movement with quick body undulations that often produce clouds of sediments uplifted from the bed. They also frequently dig into the sediment (Grothues et al. 2012). An unknown proportion of the variation in RSL was therefore caused by bioturbation by both fish, and perhaps also by other fish species that spawn their eggs within hollow rhodoliths (Gagnon et al. 2012).

Conclusions and future research directions

Knowledge about factors and processes that regulate the structure, function, and stability of rhodolith beds is limited compared to long-studied coral reef, seagrass, and kelp bed (forest) systems (Foster 2001, Kaldy & Lee 2007, Montaggioni & Braithwaite 2009, Filbee-Dexter & Scheibling 2014). As pointed out over 15 yr ago (Foster 2001) and reiterated recently (Riosmena-Rodriguez et al. 2017), the rhodolith research community needs to move from short-term, descriptive studies and qualitative correlations to long-term field studies of factors affecting rhodoliths within and at the distributional limits of beds to gain a better understanding of the causes of bed distribution and dynamics. The present study, which combines experimental testing of bioturbators' effectiveness with short (a few weeks) and longer (a few months) surveys of abiotic and biotic factors potentially affecting RSL and movement at the upper and lower limits of a major rhodolith bed in Newfoundland, is an important step in this direction. This approach provided answers to the main hypotheses about drivers of rhodolith bed stability, highlighted the key role of rhodolith cryptofauna and macrofauna in preventing accumulation of sediments on rhodoliths, and revealed the different scales (within and outside rhodoliths) at which these bioturbators operate. This is an important aspect of rhodolith bed ecology that had not previously been demonstrated.

The present study focussed on 1 rhodolith bed over a 7 mo period. Interestingly, ~38% of the spatial and temporal variation in RSL from June to December was explained by factors other than water flow. Multiyear monitoring to capture longer-term variability in water flow, including frequency and intensity of wave storms, as well as studies of the effects of press and pulse disturbances (Tompkins & Steller 2016), are needed to assess resistance and resilience of rhodolith beds to natural and anthropogenic stressors. Similar studies in other parts of Newfoundland and abroad are needed to assess the generality of the present results. More detailed studies in controlled environments are also required to determine threshold hydrodynamic forces triggering rhodolith movement and abrasion (authors' unpubl. data). Feeding relationships among rhodolith fauna and flora and their likely connections with phytoplankton and zooplankton are poorly understood, and also deserve greater attention (Hinojosa-Arango & Riosmena-Rodríguez 2004, Grall et al. 2006).

Because water motion can induce rhodolith movement while affecting sedimentation processes, it is currently considered a key determinant of rhodolith survival, and hence of the distribution, structure, and function of rhodolith beds (Bosence 1985, Scoffin et al. 1985, Marrack 1999, Hinojosa-Arango et al. 2009). Findings in the present study and in a companion study of structural aspects of the same rhodolith bed (Gagnon et al. 2012) challenge this paradigm by showing that beds can actually thrive under chronic low-level hydrodynamic forces that are insufficient to move rhodoliths. The bed in St. Philip's exhibits the characteristics of '*in situ*' beds (Bosence 1976), with no appreciable variation in rhodolith growth form and branching density, and tight clustering of rhodoliths with no signs of physical disturbance across the bed (P. Gagnon pers. obs.). It is maintained primarily by activities of select resident bioturbators, which physically move rhodoliths or live within them, preventing sediment accumulation and perhaps overgrowth. The present and a few other studies (e.g. Prager & Ginsburg 1989, Marrack 1999, James 2000, Pereira-Filho et al. 2015) speak to the importance of considering interactions among environmental variability and biogenic and environmentally driven movement of rhodoliths to better capture the range of factors and processes that control rhodolith bed stability. Rhodolith beds abound in temperate and subarctic Newfoundland and Labrador (Bosence 1983, Gagnon et al. 2012, Adey et al. 2015) and hold great promise for providing additional answers to key questions in rhodolith bed ecology.

Acknowledgements. We are grateful to D. Bélanger, A. P. St-Pierre, S. Trueman, C. Sandall, V. Battcock, and J. Lima for help with field and laboratory work, D. Schneider for statistical advice, L. Zedel for guidance on pruning and averaging of raw water flow data, and H. Penney for assistance with preparation of maps. We also thank E. Edinger, D. Robert, and 3 anonymous reviewers for constructive comments that helped improve the manuscript. This research was supported by Natural Sciences and Engineering Research Council (NSERC Discovery Grant), Canada Foundation for Innovation (CFI Leaders Opportunity Funds), Research & Development Corporation of Newfoundland and Labrador (Ignite R&D), and Department of Fisheries and Aquaculture of Newfoundland and Labrador (DFA) grants to P.G.; K.R.M. was supported by the NSERC Alexander Graham Bell Canada Graduate Scholarship Program.

LITERATURE CITED

Adey WH (1966) Distribution of saxicolous crustose corallines in the northwestern North Atlantic. J Phycol 2: 49–54

Adey WH, Adey PJ (1973) Studies on the biosystematics and ecology of the epilithic crustose Corallinaceae of the British Isles. Br Phycol J 8:343–407

Adey WH, Hayek LAC (2011) Elucidating marine biogeography with macrophytes: quantitative analysis of the North Atlantic supports the thermogeographic model and demonstrates a distinct subarctic region in the northwestern Atlantic. Northeast Nat 18:1–128

Adey WH, Chamberlain YM, Irvine LM (2005) An SEM-based analysis of the morphology, anatomy, and reproduction of *Lithothamnion tophiforme* (Esper) Unger (Corallinales, Rhodophyta), with a comparative study of associated North Atlantic Arctic/Subarctic Melobesioideae. J Phycol 41:1010–1024

Adey W, Halfar J, Humphreys A, Suskiewicz T, Bélanger D, Gagnon P, Fox M (2015) Subarctic rhodolith beds promote longevity of crustose coralline algal buildups and their climate archiving potential. Palaios 30:281–293

Amado-Filho GM, Maneveldt GW, Pereira-Filho GH, Manso RCC, Bahia RG, Barros-Barreto MB, Guimarães S (2010) Seaweed diversity associated with a Brazilian tropical rhodolith bed. Cienc Mar 36:371–391

Amado-Filho GM, Moura RL, Bastos AC, Salgado LT and others (2012) Rhodolith beds are major $CaCO_3$ bio-factories in the tropical south west Atlantic. PLOS ONE 7: e35171

Andrades R, Gomes MP, Pereira-Filho GH, Souza-Filho JF, Albuquerque CQ, Martins AS (2014) The influence of allochthonous macroalgae on the fish communities of tropical sandy beaches. Estuar Coast Shelf Sci 144:75–81

Ávila E, Riosmena-Rodríguez R, Hinojosa-Arango G (2013) Sponge-rhodolith interactions in a subtropical estuarine system. Helgol Mar Res 67:349–357

Ballantine DL, Bowden-Kerby A, Aponte NE (2000) *Cruoriella* rhodoliths from shallow-water back reef environments in La Parguera, Puerto Rico (Caribbean Sea). Coral Reefs 19:75–81

Ballesteros E (1994) The deep-water *Peyssonnelia* beds from the Balearic Islands (Western Mediterranean). Mar Ecol 15:233–253

Basso D (1998) Deep rhodolith distribution in the Pontian Islands, Italy: a model for the paleoecology of a temperate sea. Palaeogeogr Palaeoclimatol Palaeoecol 137: 173–187

Basso D, Nalin R, Nelson CS (2009) Shallow-water *Sporolithon* rhodoliths from North Island (New Zealand). Palaios 24:92–103

Blain C, Gagnon P (2013) Interactions between thermal and wave environments mediate intracellular acidity (H_2SO_4), growth, and mortality in the annual brown seaweed *Desmarestia viridis*. J Exp Mar Biol Ecol 440:176–184

Bohm L, Schramm W, Rabsch U (1978) Ecological and physiological aspects of some coralline algae from the western Baltic. Calcium uptake and skeleton formation in *Phymatolithon calcareum.* Kieler Meeresforsch 4:282–288

Bosence DWJ (1976) Ecological studies on two unattached coralline algae from Western Ireland. Palaeontology 19: 365–395

Bosence DWJ (1983) The occurrence and ecology of recent rhodoliths — a review. In: Peryt TM (ed) Coated grains. Springer-Verlag, Berlin, p 225–242

Bosence DWJ (1985) The morphology and ecology of a mound-building coralline alga (*Neogoniolithon strictum*) from the Florida Keys. Palaeontology 28:189–206

Brodie G, Porter S, Robertson A (eds) (1993) Climate and weather of Newfoundland and Labrador. Workshop on the Climate and Weather of Newfoundland and Labrador. Creative Publishing, St. John's

Burnham KP, Anderson DR (2004) Multimodel inference: understanding AIC and BIC in model selection. Sociol Methods Res 33:261–304

Cabaço S, Santos R (2007) Effects of burial and erosion on the seagrass *Zostera noltii*. J Exp Mar Biol Ecol 340: 204–212

Chen M, Ding S, Liu L, Xu D, Gong M, Tang H, Zhang C (2016) Kinetics of phosphorus release from sediments and its relationship with iron speciation influenced by the mussel (*Corbicula fluminea*) bioturbation. Sci Total Environ 542:833–840

Dahlgren CP, Posey MH, Hulbert AW (1999) The effects of bioturbation on the infaunal community adjacent to an offshore hardbottom reef. Bull Mar Sci 64:21–34

Dearborn J, Edwards K, Fratt D (1981) Feeding biology of sea stars and brittle stars along the Antarctic Peninsula. Antarct J US 16:136–137

De Boer WF (2007) Seagrass–sediment interactions, positive feedbacks and critical thresholds for occurrence: a review. Hydrobiologia 591:5–24

Drolet D, Himmelman JH, Rochette R (2004a) Use of refuges by the ophiuroid *Ophiopholis aculeata*: contrasting effects of substratum complexity on predation risk from two predators. Mar Ecol Prog Ser 284:173–183

Drolet D, Himmelman JH, Rochette R (2004b) Effect of light and substratum complexity on microhabitat selection and activity of the ophiuroid *Ophiopholis aculeata.* J Exp Mar Biol Ecol 313:139–154

Eberly L (2007) Multiple linear regression. In: Ambrosius W (ed) Topics in biostatistics. Humana Press, Totowa, NJ, p 165–187

Filbee-Dexter K, Scheibling RE (2014) Sea urchin barrens as alternative stable states of collapsed kelp ecosystems. Mar Ecol Prog Ser 495:1–25

Foster MS (2001) Rhodoliths: between rocks and soft places. J Phycol 37:659–667

Fox J, Weisberg S (2011) An R companion to applied regression, 2nd edn. Sage, Thousand Oaks, CA

Frey DL, Gagnon P (2016) Spatial dynamics of the green sea

urchin *Strongylocentrotus droebachiensis* in food-depleted habitats. Mar Ecol Prog Ser 552:223–240

Gagnon P, Matheson K, Stapleton M (2012) Variation in rhodolith morphology and biogenic potential of newly discovered rhodolith beds in Newfoundland and Labrador (Canada). Bot Mar 55:85–99

Gaymer CF, Dutil C, Himmelman JH (2004) Prey selection and predatory impact of four major sea stars on a soft bottom subtidal community. J Exp Mar Biol Ecol 313: 353–374

Graham DJ, Midgley NG (2000) Graphical representation of particle shape using triangular diagrams: an Excel spreadsheet method. Earth Surf Process Landf 25: 1473–1477

Grall J, Le Loc'h F, Guyonnet B, Riera P (2006) Community structure and food web based on stable isotopes ($\delta^{15}N$ and $\delta^{13}C$) analysis of a North Eastern Atlantic maerl bed. J Exp Mar Biol Ecol 338:1–15

Grothues TM, Able KW, Pravatiner JH (2012) Winter flounder (*Pseudopleuronectes americanus* Walbaum) burial in estuaries: acoustic telemetry triumph and tribulation. J Exp Mar Biol Ecol 438:125–136

Hall SJ (1994) Physical disturbance and marine benthic communities: life in unconsolidated sediments. Oceanogr Mar Biol Annu Rev 32:179–239

Hall-Spencer J, White N, Gillespie E, Gillham K, Foggo A (2006) Impact of fish farms on maerl beds in strongly tidal areas. Mar Ecol Prog Ser 326:1–9

Himmelman JH, Dutil C (1991) Distribution, population structure and feeding of subtidal seastars in the northern Gulf of St. Lawrence. Mar Ecol Prog Ser 76:61–72

Hinchey EK, Schaffner LC, Hoar CC, Vogt BW, Batte LP (2006) Responses of estuarine benthic invertebrates to sediment burial: the importance of mobility and adaptation. Hydrobiologia 556:85–98

Hinojosa-Arango G, Riosmena-Rodríguez R (2004) Influence of rhodolith-forming species and growth-form on associated fauna of rhodolith beds in the central-west Gulf of California, México. Mar Ecol 25:109–127

Hinojosa-Arango G, Maggs CA, Johnson MP (2009) Like a rolling stone: the mobility of maerl (Corallinaceae) and the neutrality of the associated assemblages. Ecology 90: 517–528

James DW (2000) Diet, movement, and covering behavior of the sea urchin *Toxopneustes roseus* in rhodolith beds in the Gulf of California, México. Mar Biol 137:913–923

Julien PY (2010) Erosion and sedimentation, 2nd edn. Cambridge University Press, Cambridge

Kaldy JE, Lee KS (2007) Factors controlling *Zostera marina* L. growth in the eastern and western Pacific Ocean: comparisons between Korea and Oregon, USA. Aquat Bot 87: 116–126

Kamenos NA, Moore PG, Hall-Spencer JM (2004a) Small-scale distribution of juvenile gadoids in shallow inshore waters; what role does maerl play? ICES J Mar Sci 61: 422–429

Kamenos NA, Moore PG, Hall-Spencer JM (2004b) Maerl grounds provide both refuge and high growth potential for juvenile queen scallops (*Aequipecten opercularis* L.). J Exp Mar Biol Ecol 313:241–254

Klamkin MS (1971) Elementary approximations to the area of n-dimensional ellipsoids. Am Math Mon 78:280–283

Klein JC, Verlaque M (2009) Macroalgal assemblages of disturbed coastal detritic bottoms subject to invasive species. Estuar Coast Shelf Sci 82:461–468

Kristensen E, Penha-Lopes G, Delefosse M, Valdemarsen T, Quintana CO, Banta GT (2012) What is bioturbation? The need for a precise definition for fauna in aquatic sciences. Mar Ecol Prog Ser 446:285–302

Lowe RJ, Falter JL, Bandet MD, Pawlak G, Atkinson MJ, Monismith SG, Koseff JR (2005) Spectral wave dissipation over a barrier reef. J Geophys Res Oceans 110:C04001

Marrack EC (1999) The relationship between water motion and living rhodolith beds in the southwestern Gulf of California, Mexico. Palaios 14:159–171

Martin S, Clavier J, Chauvaud L, Thouzeau G (2007) Community metabolism in temperate maerl beds. I. Carbon and carbonate fluxes. Mar Ecol Prog Ser 335:19–29

Montaggioni LF, Braithwaite CJR (2009) Quaternary coral reef systems: history, development processes and controlling factors. Elsevier, Amsterdam

Munk JE (1992) Reproduction and growth of green urchins *Strongylocentrotus droebachiensis* (Mueller) near Kodiak, Alaska. J Shellfish Res 11:245–254

Neill K, Nelson W, D'Archino R, Leduc D, Farr T (2015) Northern New Zealand rhodoliths: assessing faunal and floral diversity in physically contrasting beds. Mar Biodivers 45:63–75

Nichols D, Barker MF (1984) Growth of juvenile *Asterias rubens* L. (Echinodermata : Asteroidea) on an intertidal reef in southwestern Britain. J Exp Mar Biol Ecol 78: 157–165

Pereira-Filho GH, Francini-Filho RB, Pierozzi-Jr I, Pinheiro HT and others (2014) Sponges and fish facilitate succession from rhodolith beds to reefs. Bull Mar Sci 91:45–46

Pereira-Filho GH, Veras PC, Francini-Filho RB, de Moura RL and others (2015) Effects of the sand tilefish *Malacanthus plumieri* on the structure and dynamics of a rhodolith bed in the Fernando de Noronha Archipelago, tropical West Atlantic. Mar Ecol Prog Ser 541:65–73

Piazzi L, Pardi G, Cinelli F (2002) Structure and temporal dynamics of a macroalgal assemblage associated with a rhodolith bed of the Tuscan archipelago (Tyrrhenian Sea). Atti Soc Tosc Sci Nat Mem 109:5–10

Piller WE, Rasser M (1996) Rhodolith formation induced by reef erosion in the Red Sea, Egypt. Coral Reefs 15:191–198

Pinet PR (2000) Essential invitation to oceanography, 2nd edn. Jones and Bartlett Publishers, Boston, MA

Prager EJ, Ginsburg RN (1989) Carbonate nodule growth on Florida's outer shelf and its implications for fossil interpretations. Palaios 4:310–317

Quinn GP, Keough MJ (2002) Experimental design and data analysis for biologists. Cambridge University Press, Cambridge

R Core Team (2014) R: a language and environment for statistical computing. R Foundation for Statistical Computing, Vienna

Riosmena-Rodríguez R, López-Calderón JM, Mariano-Meléndez E, Sánchez-Rodríguez A, Fernández-Garcia C (2012) Size and distribution of rhodolith beds in the Loreto Marine Park: their role in coastal processes. J Coast Res 279:255–260

Riosmena-Rodriguez R, Nelson W, Aguirre J (eds) (2017) Rhodolith/maërl beds: a global perspective. Springer International Publishing, Basel

Riul P, Targino CH, Farias JDN, Visscher PT, Horta PA (2008) Decrease in *Lithothamnion* sp. (Rhodophyta) primary production due to the deposition of a thin sediment layer. J Mar Biol Assoc UK 88:17–19

Ryan DA, Brooke BP, Collins LB, Kendrick GA and others

(2007) The influence of geomorphology and sedimentary processes on shallow-water benthic habitat distribution: Esperance Bay, Western Australia. Estuar Coast Shelf Sci 72:379–386

Scheffer M, Portielje R, Zambrano L (2003) Fish facilitate wave resuspension of sediment. Limnol Oceanogr 48: 1920–1926

Scheibling R, Hatcher B (2007) Ecology of *Strongylocentrotus droebachiensis*. In: Lawrence J (ed) Edible sea urchins: biology and ecology. Elsevier, Amsterdam, p 353–392

Scheibling RE, Metaxas A (2008) Abundance, spatial distribution, and size structure of the sea star *Protoreaster nodosus* in Palau, with notes on feeding and reproduction. Bull Mar Sci 82:221–235

Schneider CA, Rasband WS, Eliceiri KW (2012) NIH Image to ImageJ: 25 years of image analysis. Nat Methods 9: 671–675

Sciberras M, Rizzo M, Mifsud J, Camilleri K, Borg J, Lanfranco E, Schembri P (2009) Habitat structure and biological characteristics of a maerl bed off the northeastern coast of the Maltese Islands (central Mediterranean). Mar Biodivers 39:251–264

Scoffin T, Stoddart D, Tudhope A, Woodroffe C (1985) Rhodoliths and coralliths of Muri Lagoon, Rarotonga, Cook Islands. Coral Reefs 4:71–80

Singer JD, Willett JB (2003) Applied longitudinal data analysis: modeling change and event occurrence. Oxford University Press, Oxford

Smith NP (1994) Long-term Gulf-to-Atlantic transport through tidal channels in the Florida Keys. Bull Mar Sci 54:602–609

Snedecor GW, Cochran WG (1994) Statistical methods, 8th edn. Iowa State University Press, Ames, IA

Sneed ED, Folk RL (1958) Pebbles in the lower Colorado River, Texas; a study in particle morphogenesis. J Geol 66:114–150

Sokal RR, Rohlf FJ (2012) Biometry: the principles and practice of statistics in biological research. WH Freeman and Co, New York, NY

St-Pierre A, Gagnon P (2015) Effects of temperature, body size, and starvation on feeding in a major echinoderm predator. Mar Biol 162:1125–1135

Steller DL, Caceres-Martinez C (2009) Coralline algal rhodoliths enhance larval settlement and early growth of the Pacific calico scallop *Argopecten ventricosus*. Mar Ecol Prog Ser 396:49–60

Steller DL, Foster MS (1995) Environmental factors influencing distribution and morphology of rhodoliths in Bahía Concepción, B.C.S., México. J Exp Mar Biol Ecol 194: 201–212

Steller DL, Riosmena-Rodriguez R, Foster MS, Roberts CA (2003) Rhodolith bed diversity in the Gulf of California: the importance of rhodolith structure and consequences of disturbance. Aquat Conserv 13:S5–S20

Steller DL, Foster MS, Riosmena-Rodriguez R (2009) Living rhodolith bed ecosystems in the Gulf of California. In: Johnson JM, Ledesma-Vázquez J (eds) Atlas of coastal ecosystems in the Gulf of California: past and present. University of Arizona Press, Tucson, AZ, p 72–82

Stocker TF, Qin D, Plattner GK, Tignor SK and others (eds) (2014) Climate change 2013: the physical science basis. Working group I contribution to the Fifth Assessment Report of the Intergovernmental Panel on Climate Change. Cambridge University Press, Cambridge

Storlazzi CD, Field ME, Bothner MH (2011) The use (and misuse) of sediment traps in coral reef environments: theory, observations, and suggested protocols. Coral Reefs 30:23–38

Thomsen MS, McGlathery K (2006) Effects of accumulations of sediments and drift algae on recruitment of sessile organisms associated with oyster reefs. J Exp Mar Biol Ecol 328:22–34

Thomson RE, Emery WJ (2014) Data analysis methods in physical oceanography, 3rd edn. Elsevier, Amsterdam

Tompkins PA, Steller DL (2016) Living carbonate habitats in temperate California (USA) waters: distribution, growth, and disturbance of Santa Catalina Island rhodoliths. Mar Ecol Prog Ser 560:135–145

Tsuji Y (1993) Tide influenced high energy environments and rhodolith-associated carbonate deposition on the outer shelf and slope off the Miyako Islands, southern Ryukyu Island Arc, Japan. Mar Geol 113:255–271

Twichell DC, Cross VA, Peterson CD (2010) Partitioning of sediment on the shelf offshore of the Columbia River littoral cell. Mar Geol 273:11–31

Venables WN, Ripley BD (2002) Modern applied statistics with S, 4th edn. Springer, New York, NY

White J (1990) The use of sediment traps in high-energy environments. Mar Geophys Res 12:145–152

Wilcox RR (2011) Introduction to robust estimation and hypothesis testing, 3rd edn. Elsevier Science, St. Louis, MO

Wilson S, Blake C, Berges JA, Maggs CA (2004) Environmental tolerances of free-living coralline algae (maerl): implications for European marine conservation. Biol Conserv 120:279–289

Wright LD, Friedrichs CT, Kim SC, Scully ME (2001) Effects of ambient currents and waves on gravity-driven sediment transport on continental shelves. Mar Geol 175: 25–45

Editorial responsibility: Lisandro Benedetti-Cecchi, Pisa, Italy

Submitted: September 18, 2017; Accepted: January 26, 2018
Proofs received from author(s): April 12, 2018